Synchronization and detection of binary data in free-space optical communication systems using Haar wavelet transformation

Nader Namazi
Catholic University of America
Department of Electrical Engineering and Computer Science
Washington, D.C. 20064
E-mail: namazi@cua.edu

Harris Rayvon Burris Jr., MEMBER SPIE
Research Support Instruments, Inc.
Lanham, Maryland 20706

Charles Conner
Catholic University of America
Department of Electrical Engineering and Computer Science
Washington, D.C. 20064

G. Charmaine Gilbreath, MEMBER SPIE
Naval Research Laboratory
Washington, D.C. 20375

Abstract. A new method is presented to perform bit synchronization and detection of binary nonreturn-to-zero (NRZ) data from a free-space optical (FSO) communication link. Based on the wavelet transformation, a new bandpass filter is developed and implemented. It is shown that the Haar wavelet is an excellent choice for this purpose. The center frequency of this filter is a function of the scale and could be adjusted to adapt to the variation of the channel. The output of the filter is zero mean and is closely related to the derivative of the binary data. The filter has a linear phase; therefore, its output is used for synchronization and detection of the data. Analysis of the method is presented using Fourier transformation. In addition, adaptive Wiener filtering is utilized to reduce the effect of the additive white Gaussian noise in the data. Simulation experiments are performed and presented using real and synthetic data. The results of the experiments indicate that the Haar wavelet transform and adaptive Wiener filtering are robust and effective tools in dealing with FSO data. [DOI: 10.1117/1.2162029]

Subject terms: free-space optical communication; detection; wavelet transformation; Haar wavelet; adaptive Wiener filter; bit error; synchronization.

Paper 040725R received Oct. 7, 2004; revised manuscript received May 11, 2005; accepted for publication Jun. 8, 2005; published online Jan. 24, 2006. This paper is a revision of a paper presented at the SPIE Conference on Optical Science and Technology Conference, Denver, CO, August 2004. The paper presented there appears (unrefereed) in SPIE Proceedings Vol. 5550.

1 Introduction

Free-space optical (FSO) communication is an important area of research due to its advantages of providing a very large bandwidth and relatively low cost of implementation. These systems have many desirable applications, perhaps the most important of which is their use in providing a connection from the high bandwidth fiber optic backbone to the buildings and businesses desiring high bandwidth access without the high cost of installing fiber through the local infrastructure. FSO communication systems also have advantages over the free-space rf (FSRF) systems such as no frequency allocation requirements and low probability of interception and detection for covert applications.

Bit rates of FSO systems are approaching 100 Gbits/sec in the laboratory.[1–3] However, atmospheric propagation effects cause the FSO channel to be 'bursty' in nature and highly variable with a rate of change as high as 1 kHz and with power fades greater than 10 dB. Therefore, because of the very high bit rate and a time-varying channel, the bit error reduction is a difficult and vital area of research.

The motivation for the work presented in this research originated from the field testing of a multiple quantum-well, modulating retroreflector (MRR) used for fairly low data rate (less than 100 Mbps), one way, optical communications.[4] The MRR, which was developed by the U.S. Naval Research Laboratory (Washington, DC), was being tested over a two-kilometer ship-to-shore communication link. The MRR device has a relatively low contrast ratio ($\sim$3), and the combination of atmospheric turbulence in the channel and boat motion resulted in a widely varying average-received power level in the return signal. The varying average power of the received signal was beyond the capability of the amplifier ac coupling to effectively clamp to a mean of zero. The fact that the signal mean was sometimes significantly above or below the zero level made bit error rate testing *in situ* with existing equipment impossible. To determine the quality of the one-way, modulating retroreflector lasercom link, several long waveforms of both alternating ones and zeroes as well as pseudo-random bit sequences were oversampled (by approximately 10 to 1), digitized, and stored for postprocessing. The purpose of this work is to introduce and implement an effective method to deal with these issues.

In a typical RF digital communication problem, the binary data are designed to avoid intersymbol interference (ISI) and are digitally modulated. Here, the channel is, in general, modeled as bandlimited, additive, white, Gaussian noise (AWGN), and the demodulated data consist of a string of pulses with constant power. The value of the mean is typically zero, and the variance of the data is a constant. The detection problem, therefore, is to use matched filtering and constant thresholding to identify the digital data. In contrast, the FSO communication channels can be modeled

0091-3286/2006/$22.00 © 2006 SPIE

Report Documentation Page

Form Approved
OMB No. 0704-0188

1. REPORT DATE	2. REPORT TYPE	3. DATES COVERED
JAN 2006		**00-00-2006 to 00-00-2006**

4. TITLE AND SUBTITLE	5a. CONTRACT NUMBER
Synchronization and detection of binary data in free-space optical communication systems using Haar wavelet transformation	5b. GRANT NUMBER
	5c. PROGRAM ELEMENT NUMBER
6. AUTHOR(S)	5d. PROJECT NUMBER
	5e. TASK NUMBER
	5f. WORK UNIT NUMBER
7. PERFORMING ORGANIZATION NAME(S) AND ADDRESS(ES) **Naval Research Laboratory,Center for High Assurance Computer Systems,4555 Overlook Avenue, SW,Washington,DC,20375**	8. PERFORMING ORGANIZATION REPORT NUMBER
9. SPONSORING/MONITORING AGENCY NAME(S) AND ADDRESS(ES)	10. SPONSOR/MONITOR'S ACRONYM(S)
	11. SPONSOR/MONITOR'S REPORT NUMBER(S)

12. DISTRIBUTION/AVAILABILITY STATEMENT
Approved for public release; distribution unlimited

13. SUPPLEMENTARY NOTES
The original document contains color images.

14. ABSTRACT

15. SUBJECT TERMS

16. SECURITY CLASSIFICATION OF:			17. LIMITATION OF ABSTRACT	18. NUMBER OF PAGES	19a. NAME OF RESPONSIBLE PERSON
a. REPORT	b. ABSTRACT	c. THIS PAGE			
unclassified	**unclassified**	**unclassified**		**13**	

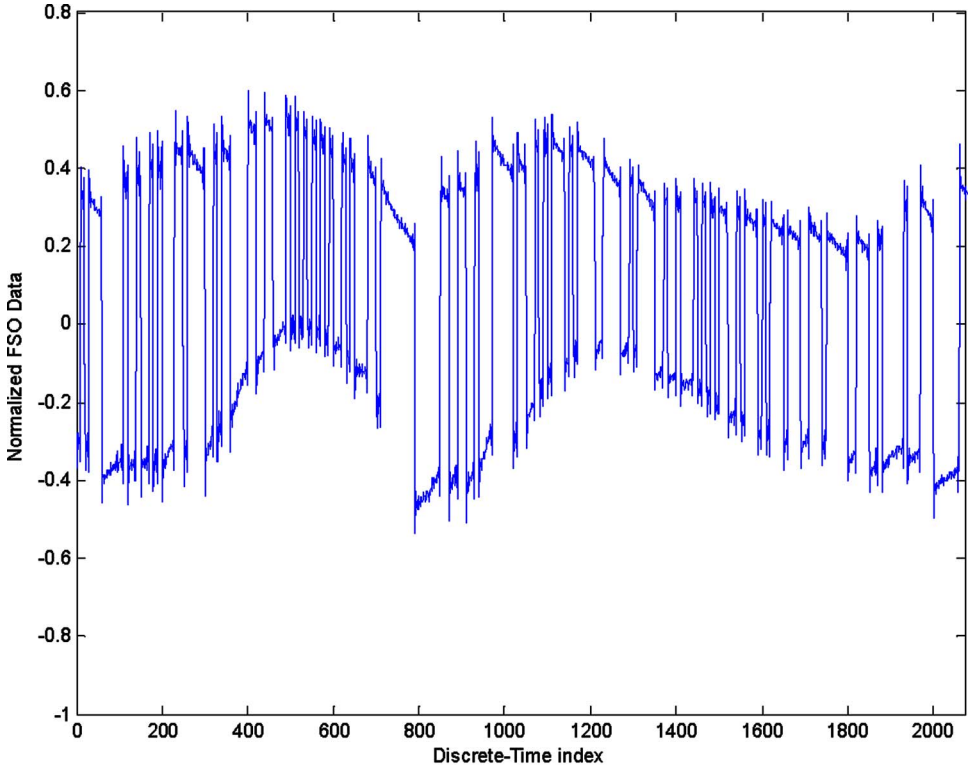

Fig. 1 Typical received FSO data.

as wideband and time-varying systems. A frequently used format of the binary data is NRZ-L[5] ("one" is represented by level +1 and "zero" is represented by level −1) with no sinusoidal modulation. The received FSO signal consists of high frequency data, which is varying in its amplitude. This corresponds to nonstationary data with variable and irregular values of mean and variance. Consequently, the conventional matched filtering and constant thresholding is often insufficient to adequately detect the data with minimum bit error rate. Figure 1 displays a typical received FSO signal. This figure shows that the binary data are a noise-like signal with variable variance and mean. It can be seen in Fig. 1 that the atmospheric turbulence and boat motion cause the received data to be widely varying in amplitude and mean. In addition, the variable power levels of the bits result in a variable bit variance due to the signal-dependent shot noise. The data can be viewed as a high frequency signal modulating a relatively much lower frequency waveform.

In this work, a new method is presented to perform the synchronization and detection of the binary data from the FSO signal. Based on the wavelet transformation, a new bandpass filter is developed and implemented. It is shown that the Haar wavelet is an excellent choice for this purpose. The center frequency of this filter is a function of the scale and could be adjusted to adapt to the variation of the channel. The output of the filter is zero mean and closely follows the derivative of the binary data. The filter has a linear phase; therefore, its output is used for synchronization and detection of the data. Analysis of the method is presented using Fourier transformation. In addition, adaptive Wiener filtering is utilized to reduce the effect of the additive white Gaussian noise in the data. Finally, it is emphasized that analysis in this work is presented for continuous-time data. However, it is assumed that the data are registered and collected in sampled form for the purpose of digital computation; consequently, the sampling issues are also taken into account.

2 Mathematical Modeling of Received Free-Space Optical Signal

The received FSO data can be mathematically described as follows:

$$r(t) = \sigma(t)d(t) + m(t) + w(t), \tag{1}$$

where t characterizes the continuous time, $d(t)$ represents the binary data, and $\sigma(t)$ signifies the variation of the signal amplitude due to atmospheric transmission effects. In addition, the model assumes two types of additive noise. The first noise $m(t)$ stands for the relatively low-frequency fluctuations of the signal mean value caused by insufficient ac coupling. The second term $w(t)$ characterizes the additive white Gaussian noise (AWGN) with zero mean. It is noted that

$$E\{r(t)\} = E\{\sigma(t)d(t)\} + E\{m(t)\}, \tag{2}$$

where $E\{.\}$ is the expectation operator, and it is assumed that $\sigma(t)d(t)$ and $m(t)$ are statistically independent. It is further assumed that $\sigma(t)$ and $d(t)$ are statistically uncorrelated, and $d(t)$ is zero mean, hence,

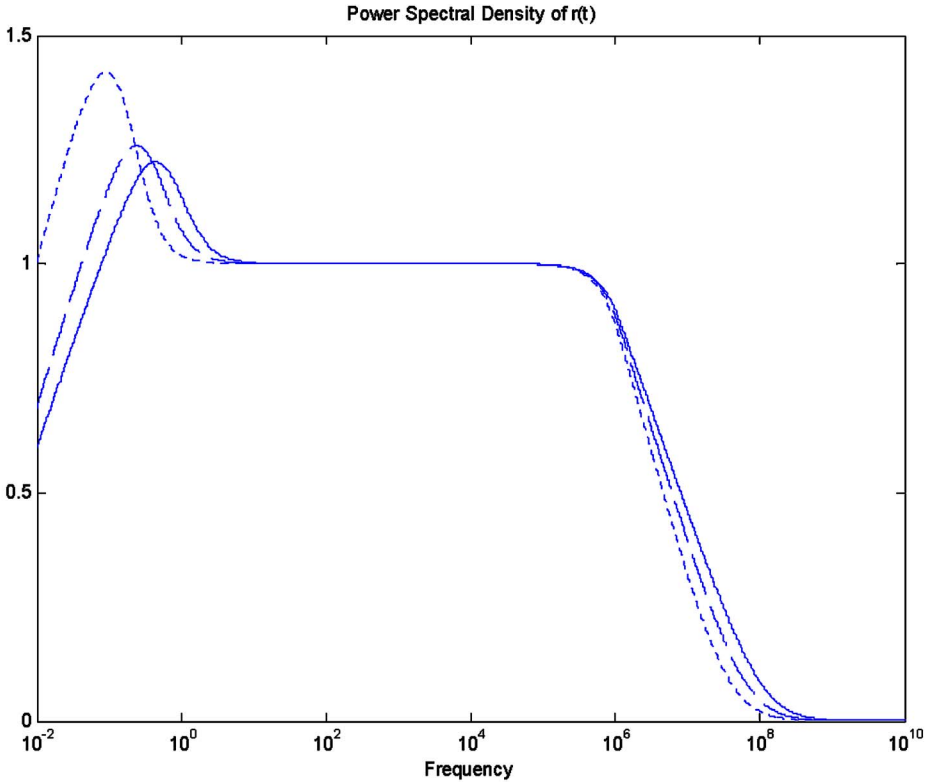

Fig. 2 The PSD of $r(t)$ versus frequency for various values of α and β, (α=.51, β=.22) for the highest peak, (α=.91, β=.51) for the mid peak, (α=1.6, β=.91) for the lowest peak.

$$E\{r(t)\} = E\{m(t)\}. \tag{3}$$

It is recognized that if $E\{m(t)\} \approx m(t)$, then in the absence of $w(t)$, we have

$$E\{[r(t) - E\{r(t)\}]^2\} = E\{\sigma^2(t)d^2(t)\}. \tag{4}$$

If the format of the data $d(t)$ is NRZ-L, then $d^2(t)=1$ and, as a result, Eq. (4) becomes

$$E\{[r(t) - E\{r(t)\}]^2\} = E\{\sigma^2(t)\}. \tag{5}$$

Consequently, when $E\{\sigma^2(t)\} \approx \sigma^2(t)$, the random process $\sigma(t)$, in the absence of $w(t)$, is a measure of the standard deviations.

3 Analysis of Free-Space Optical Signal in Frequency Domain

We now consider the FSO signal in frequency domain. It is noted that the spectrum of the white noise $w(t)$ is flat, therefore, without loss of generality, assume that $w(t)=0$. To begin, find the power spectral density (PSD) of Eq. (1),

$$S_r(\omega) = \frac{1}{2\pi} S_\sigma(\omega) * S_d(\omega) + S_m(\omega), \tag{6}$$

where $*$ represents the convolution operation and S indicates the PSD of its subscript. We assume that the data are NRZ-L, hence[6]:

$$S_d(\omega) = T_b \frac{\sin^2(\omega T_b/2)}{(\omega T_b/2)^2}, \tag{7}$$

where T_b is the bit time. To pursue the analysis, model the random processes $\sigma(t)$ and $m(t)$ by stationary, first-order Markov processes with the respective covariance functions

$$R_\sigma(\tau) = \zeta \exp(-\alpha|\tau|), \tag{8}$$

and

$$R_m(\tau) = \mu \exp(-\beta|\tau|), \tag{9}$$

where $\alpha>0$, $\beta>0$ are parameters with which the respective frequency contents of $\sigma(t)$ and $m(t)$ can be tuned; higher values of α, β correspond to higher frequency contents, and lower values are indicative of the fact that the processes are relatively slowly varying. The PSD of $\sigma(t)$ and $m(t)$ can be obtained by finding the Fourier transform of Eqs. (8) and (9); that is,

$$S_\sigma(\omega) = \frac{2\alpha\zeta}{\omega^2 + \alpha^2}, \tag{10}$$

and

$$S_m(\omega) = \frac{2\beta\mu}{\omega^2 + \beta^2}. \tag{11}$$

Application of Eqs. (11), (10), and (7) in Eq. (6) yields the PSD of $r(t)$. Figure 2 illustrates the PSD of $r(t)$ for data with the bit rate of 250 Kbps and various values of α and β. This figure shows that while the lower portion of the spectrum (close to dc) and the higher portion of the spectrum of $r(t)$ are rather sensitive to the variations of α and β, the spectrum is rather insensitive to the disparities of α and β in the midrange frequencies. By virtue of this fact, we can design a bandpass filter (BPF) in the receiver to operate in the range of frequencies for which the spectrum is relatively invariant to α and β. In the following section, it is shown that the Haar wavelet transformer, viewed as a frequency-selective filter, is a feasible choice.

4 Haar Wavelet Transformer in the Free-Space Optical Receiver

This section is concerned with the introduction and implementation of a new BPF in the receiver to generate a signal for the purpose of synchronization and detection. In addition, due to the nonstationarity of the channel, the filter should be adaptive to accommodate the variation of the channel. Furthermore, the filter must have linear phase response. We now show that the Haar wavelet transformer, viewed as a frequency-selective filter, provides these properties.

The continuous-time wavelet transform (CWT) of $r(t)$ is defined as[7]

$$W(a,b) = \frac{1}{\sqrt{|a|}} \int_{-\infty}^{\infty} r(t)\psi^*\left(\frac{t-b}{a}\right)dt, \tag{12}$$

where a and b are real parameters referred to as the scale and the time shift, respectively. In addition, the function $\psi(t)$ is called the mother wavelet. For the sake of our discussion, it suffices to rewrite Eq. (12) as a convolution operation; that is,

$$W(a,b) = r(b) * \frac{1}{\sqrt{|a|}}\psi^*\left(\frac{-b}{a}\right). \tag{13}$$

This implies that, for any scale a, the wavelet coefficient $W(a,b)$ is the output of a continuous-time, linear, time-invariant (CTLTI) filter with impulse response

$$h(t;a) = \frac{1}{\sqrt{|a|}}\psi^*\left(\frac{-t}{a}\right), \tag{14}$$

and input $r(t)$. We now consider the Haar mother wavelet described as follows[7]:

$$\psi(t) = u(t) - 2u\left(t - \frac{1}{2}\right) + u(t-1), \tag{15}$$

where $u(t)$ is the unit-step function. The Haar mother wavelet is displayed in Fig. 3. It follows from Eqs. (14) and (15) that the frequency response of the Haar filter is

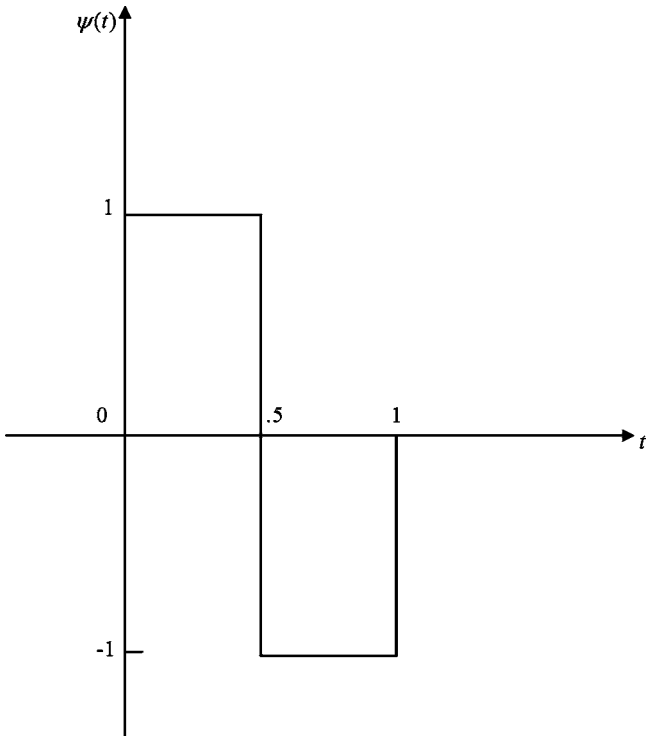

Fig. 3 Haar mother wavelet described in Eq. (15).

$$H(j\omega;a) = -j\sqrt{|a|}\left\{\frac{\sin^2\frac{a\omega}{4}}{\frac{a\omega}{4}}\right\}\exp(ja\omega/2). \tag{16}$$

This is a finite impulse response (FIR) bandpass filter with linear phase. It follows from Eq. (16) that the frequency of the highest peak of the magnitude of $H(j\omega;a)$ is a function of the scale a; that is,

$$\omega_p \cong 4.7/a. \tag{17}$$

Equation (17) implies that we can shift the filter in the frequency domain by varying the scale a. Figure 4 depicts the magnitude response of the Haar filter in Eq. (16) for $a=15T_s$, $a=8T_s$, $a=5T_s$, and $a=3T_s$, where T_s is the sampling time. This figure illustrates that the Haar filter is indeed a bandpass filter whose spectrum moves to the left as the scale is increased. This property can be used to set and adjust the scale to adapt to the variation of the channel.

The receiver filter is assumed to be

$$G(j\omega;a) = -H(j\omega;a). \tag{18}$$

The input of this filter is $r(t)$ and the output of the filter is $x(t)$. In view of Eqs. (6), (7), (10), (11), (16), and (18), it follows that the PSD of $x(t)$ becomes

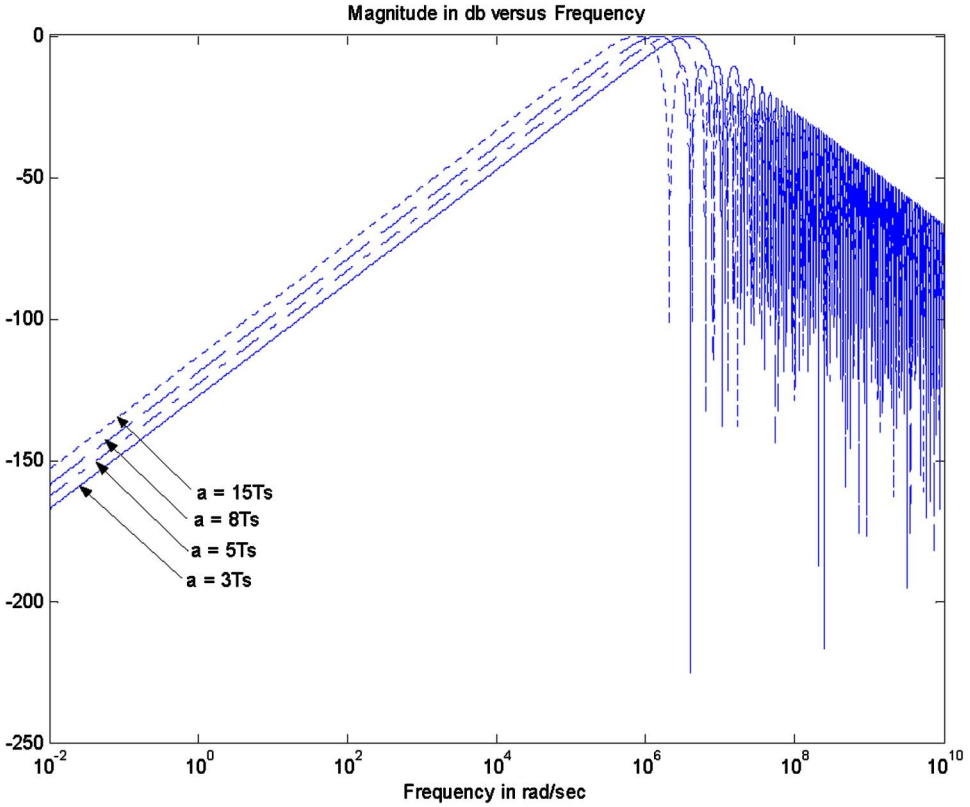

Fig. 4 Magnitude frequency response of the Haar filter in Eq. (16) for various values of scale a as a function of the sampling interval T_s.

$$S_x(\omega;a)=\frac{|a|T_b}{2\pi}\left\{\frac{\sin^2\frac{a\omega}{4}}{\frac{a\omega}{4}}\right\}^2\left\{\left[\frac{2\alpha\zeta}{\omega^2+\alpha^2}\right]*\frac{\sin^2(\omega T_b/2)}{(\omega T_b/2)^2}\right\}+|a|\left\{\frac{\sin^2\frac{a\omega}{4}}{\frac{a\omega}{4}}\right\}^2\left\{\frac{2\beta\mu}{\omega^2+\beta^2}\right\}. \quad (19)$$

It is observed from Eq. (19) that $S_x(\omega)$ consists of two terms that are affected by the filter in Eq. (18). Notice that by the appropriate choice of the scale a, we can considerably reduce the second term. This stems from the fact that the low-pass spectrum of $S_m(\omega)$ is multiplied by a bandpass spectrum of Eq. (18). The optimum choice of the scale can cause a minimum overlap between the two spectra, which in turn results in the filtering of the average term $m(t)$. It should be mentioned that there is a tradeoff in the selection of the scale. On one hand, small values of the scale, below a boundary, increase the resolution and results in a noisy output signal. Clearly, this results into erroneous decision of the binary data. On the other hand, increasing the scale beyond a limit can lead to the overlap of the spectrum of the filter in Eq. (18) and $S_m(\omega)$, which leads to an alias of the average term in the output of the filter. This results in complications in setting the detection threshold of the binary data. Therefore, there is a range of scale that should be used for the best performance of the filter in Eq. (18) for the removal of $m(t)$.

The choice of the scale also affects the first term of Eq. (19). This term constitutes the filtering of a signal that is the result of the convolution process of a low-pass waveform $\sigma(t)$ with a relatively much wider band signal $d(t)$. The filter shown in Eq. (18), depending on its scale-dependent frequency band, selects a portion of the spectrum of the convolved signal. The result is subsequently used for synchronization and detection of the binary data $d(t)$.

5 Synchronization and Detection of Filtered Free-Space Optical Data

The first step after the filtering of Eq. (18) is the synchronization process. Synchronization is an important step in any digital communication system. Various levels of synchronization are usually required such as bit, word, frame, network, clock, etc. Here we focus on establishing a new method for bit synchronization (timing recovery) of FSO communication data.

There are many techniques to accomplish synchronization in an FSO communication system. For example, Ref. 8 discusses four-bit synchronization techniques for an APD-based, direct detection optical communication system with on-off modulation over a nonfading channel. The methods reported in Ref. 8 require a nonlinear circuit element to generate a discrete frequency component at the clock frequency, which is then passed through a bandpass filter and sent to a zero-crossing detector to generate a clock wave-

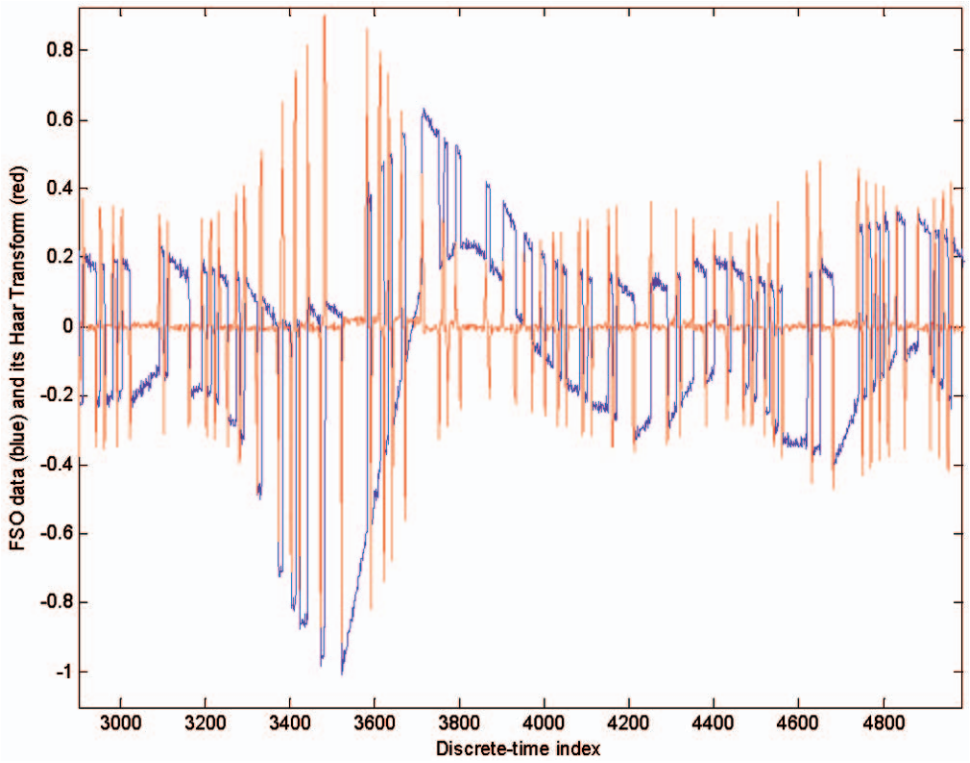

Fig. 5 A portion of received FSO data (blue) with its corresponding Haar transform (red).

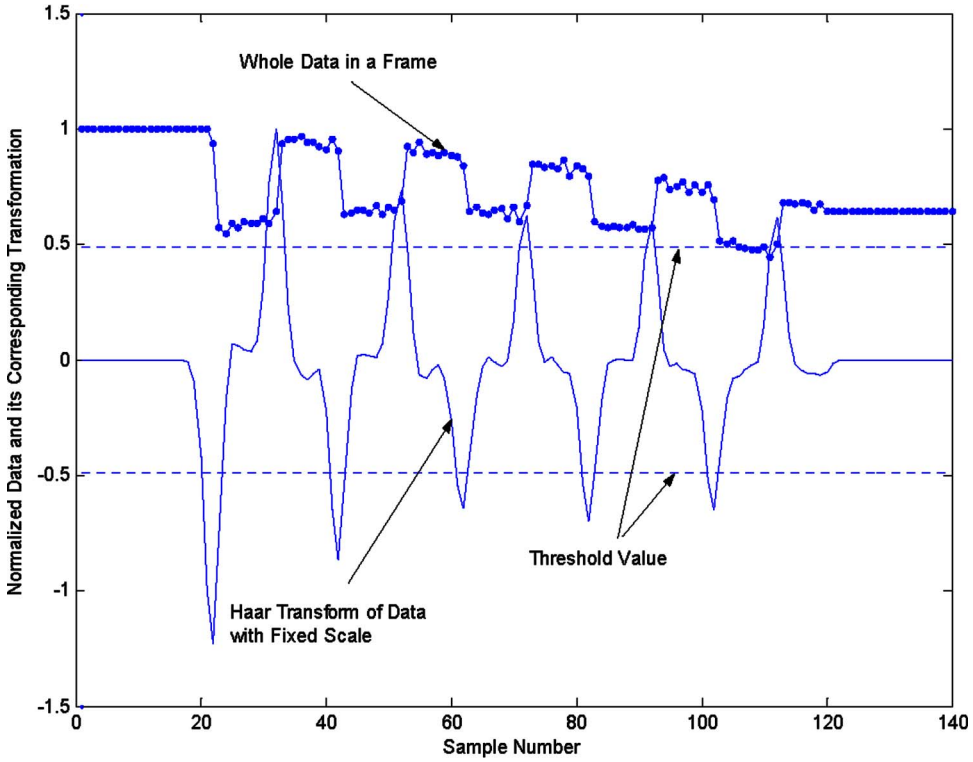

Fig. 6 A frame of data with modified boundary values.

form. The major advantage of the Haar filter introduced in this work over the traditional methods is that the output of the Haar filter is a suitable signal that can be used for joint synchronization and detection of binary data. In addition, the Haar filter effectively eliminates the need for any nonlinear circuit element, and replaces the bandpass filter introduced in traditional schemes.

The FSO signal in this work is assumed to be in sampled format. Typically, we have $N \geqslant 1$ samples per bit. However, due to the fact that the digitizer clock is not synchronized to the beginning of the bit pulse, some bits will have a lesser number of samples than N. Hence, we need a method to synchronize to the start of each bit to "integrate" over the bit period for bit detection. Figure 5 highlights a scenario for which real data from the MRR FSO link is used. The receiver filter in Eq. (18) is assumed to have the scale $a = 5T_s$, where T_s is the sampling interval. This figure shows that the filter generates a sequence of zero-mean pulses at the exact bit transitions. This figure also highlights the fact that the filter in Eq. (18) approximates a differentiation of the data with each short pulse following the upward and downward direction of $d(t)$. This fact can be further justified by finding the rectangular pulse response of Eq. (18) using a convolution process. It is seen that if the width of the input pulse is T_b and the scale $a < T_b$, the pulse response of the filter in Eq. (18) consists of two short spikes in the direction of the pulse transitions. The location of these pulses as well as their signs can be used to jointly synchronize and detect the data.

It is observed from Fig. 5 that the small values of CWT between the two consecutive peaks are tuned with the fact that the last bit has not changed. Also, once a peak occurs, the next one must have an opposite sign to represent a change. In other words, two consecutive peaks with the same sign are an indication of the detection error(s).

The detection of the data is accomplished on a frame-by-frame basis. For each frame, the wavelet transform is obtained using the Haar transformation with a fixed scale. It is relevant to mention that due to the frame-by-frame processing of the data, the transformed signal exhibits an oscillatory behavior, commonly referred to as the Gibbs phenomenon.[9] This results in an erroneous decision in the bit detection at the beginning and end of the block. To circumvent the problem, prior to the Haar transformation, the leading and trailing samples of the received data are extended by several bit intervals to the right and left, respectively. This extension tends to protect the data from erroneous changes caused by the boundary points. The maximum peak of the transformed frame is then searched and identified. If a significant maximum value is detected, its location is designated as the beginning of a bit and is used to generate two sequences, namely, the sequence to the right of the maximum, referred to as the "right data," and the sequence to the left of the maximum, signified as the "left data." (In the event for which all bits within a frame are the same, the transformed data is relatively small and no significant maximum value will be detected. A possible approach is to extend the last bit of the previous frame over the entire current frame and proceed to the following frame. Another method is to increase the length of the current frame as long as a major maximum is observed.) The right and the left data are independently processed as follows. For each sequence, a ternary sequence with the values of $\{-1, 0, +1\}$ is formed; the peaks over and below two

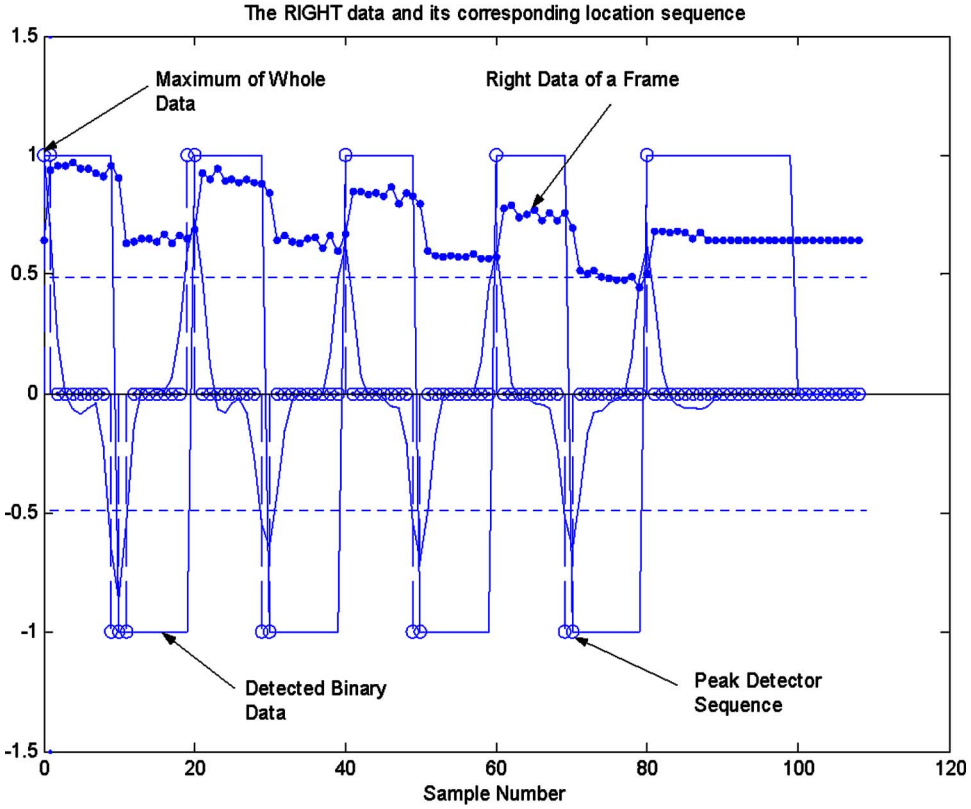

Fig. 7 A "right data" and its corresponding location sequence.

predefined threshold levels are mapped into +1 and −1, respectively: and the values within these threshold values are mapped into 0's. It is noted that the location of the appreciable peaks are expected to be at the multiple integers of a bit sample number. This fact can be used to consolidate the consecutive +1's and −1's into single +1's and −1's at these locations. The bit detection for the data is then accomplished from the ternary data. If a 1 is detected followed by 0's, the high bit starts and stays over the duration of the zeros. Accordingly, if a −1 is detected pursued by 0's, the low bit starts and is maintained over the period of 0's. It is noted that the right data always starts with a high bit and the left data, viewed backward in time, always begins with a low bit. After the bit detection is accomplished for the left and right sequences, the results are attached and truncated to the original length of the frame. The whole process is then repeated for the subsequent frames.

6 Simulation Experiments

In this section, we present the results of two experiments. The first experiment deals with the synchronization and detection of a binary sequence using real, experimentally obtained FSO data. The data were acquired at the Naval Research Laboratory's Maritime Free-Space Lasercom Test Facility at Chesapeake Beach, Maryland, from a modulating retroreflector link.[4] In the second experiment, we present a synthetic scenario to study the sensitivity of the algorithm to the AWGN noise term $w(t)$. In both experiments, every frame was extended by two-bit time intervals to the right and left to reduce the windowing effect. We used the Haar wavelet transformations of the received data with the scales over the range $[3T_s:6T_s]$ with increments of $0.2T_s$. The transformed signals were then averaged and smoothed to form a single ternary waveform.

6.1 *Experiment 1*

This experiment presents the results of the implementation of the algorithm using real received data from an FSO channel. The algorithm was implemented to perform bit synchronization and bit detection over 92,754 frames of data with 10 bits per frame. The data were 250 kbps, alternating ±1 rectangular waveform, with the sampling rate of 2.5 Msamples/s. This corresponds to 3.7102 sec of the data. The experimental digitized and saved data were produced with a FireBERD 6000 bit error rate tester as the pattern generator for the free-space modulating retroreflector communications link. Patterns of alternating 1's and 0's (i.e., a square wave) and of a pseudo-random bit sequence (PRBS) were transmitted over the FSO link, oversampled, digitized, and saved for postprocessing. However, we have been unable to reproduce the PRBS sequence of the FireBERD pattern generator mathematically so that we cannot perform postprocessed bit error rate (BER) testing with the PRBS data. Therefore, the saved square wave data were used to test the BER capability of the algorithm. From inspection of short segments of the data, the algorithm appears to work very well with the PRBS data. An example of the wavelet transform performance with a PRBS sequence is shown in Fig. 5. The square wave data were originally generated to facilitate initial postprocessing algorithm de-

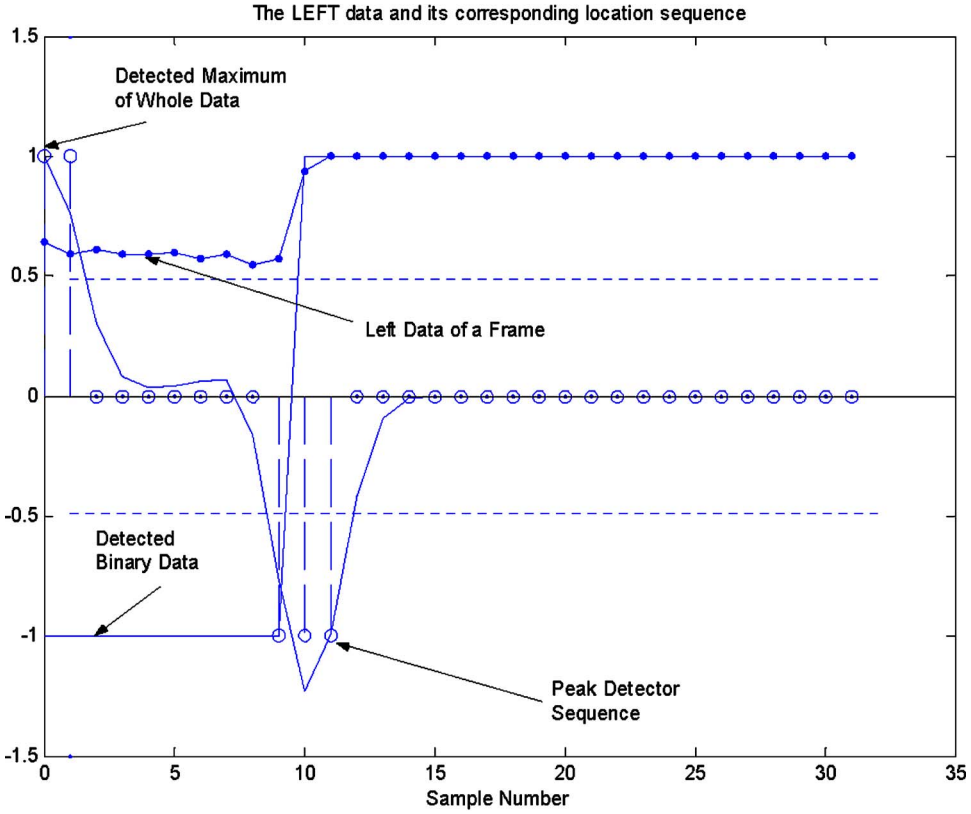

Fig. 8 A "left data" and its corresponding location sequence.

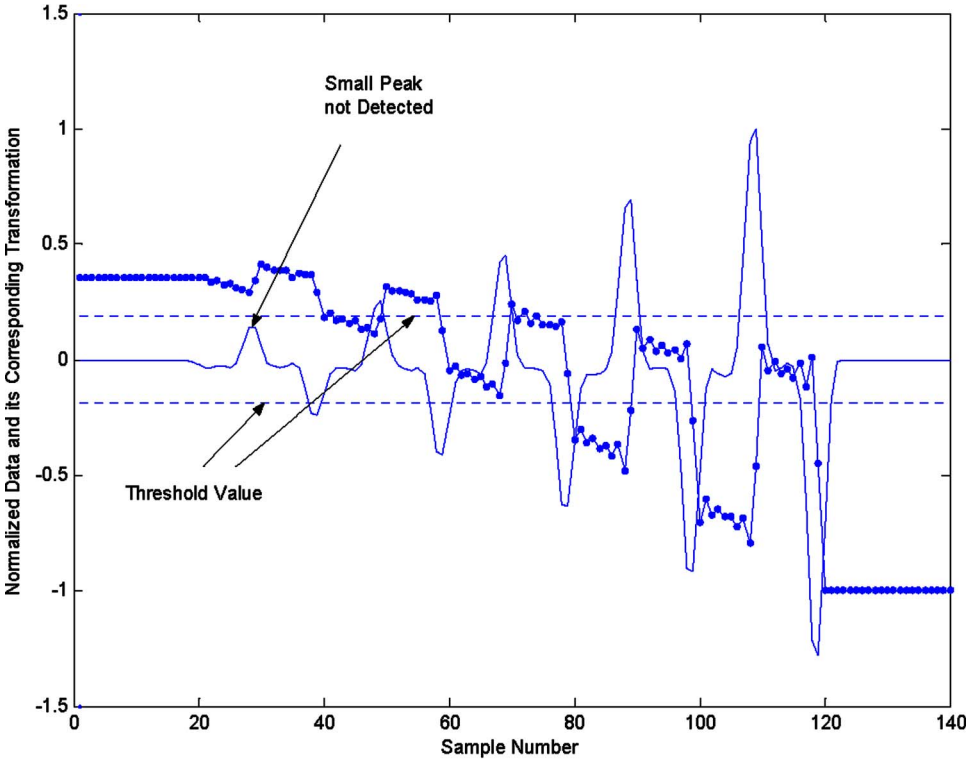

Fig. 9 The frame of data with a single detected bit error.

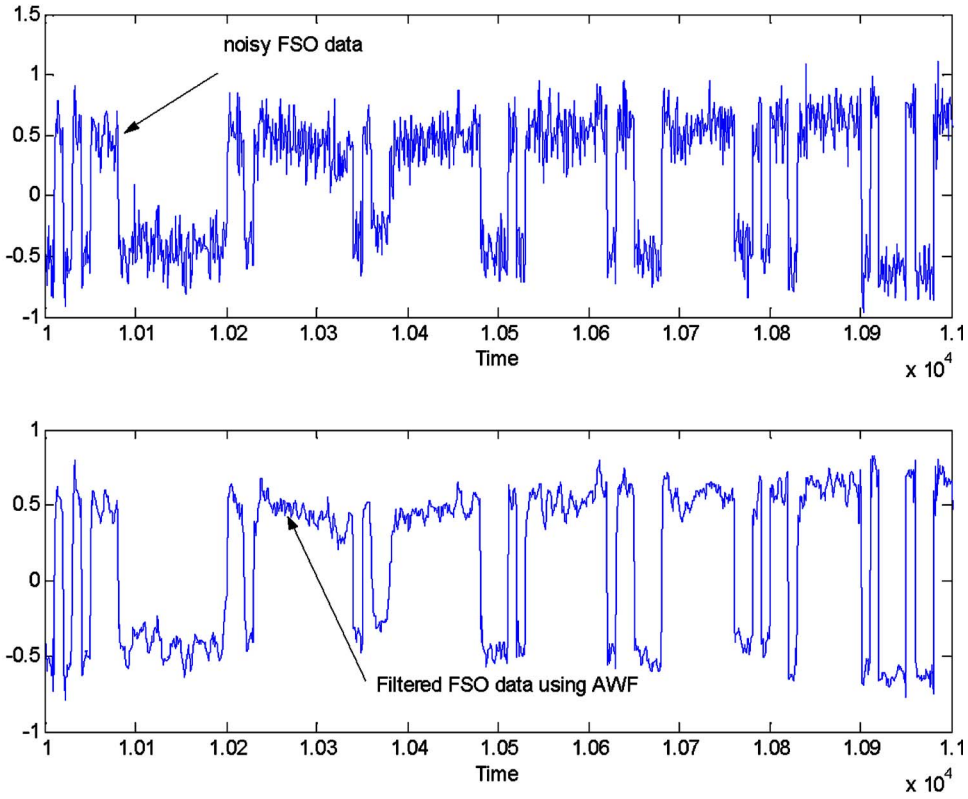

Fig. 10 A portion of the noisy FSO synthetic data (top) and its corresponding filtered version (bottom) with DSNR=10 dB and N=5 samples.

velopment for synchronization and detection. Since the PRBS pattern could not be reproduced, it also allowed some BER testing, even though the PRBS sequence would be a better indicator of the true BER performance.

Figure 6 illustrates a frame of the square wave data before being partitioned into two sequences. Figures 7 and 8 depict the respective right and left data corresponding to the frame shown in Fig. 6. The ternary sequences with the values of $\{-1,0,+1\}$ are also illustrated in these figures. The bit error for this experiment was 1.0781e-006. This corresponds to a single error over 927,540 bits of detected binary data. Figure 9 shows the frame with a single bit error. This figure shows that the first peak is below the assumed threshold value, which clearly results in a single bit error.

6.2 *Experiment 2*

This experiment presents the results of a synthetic scenario to study the sensitivity of the algorithm to the AWGN noise $w(t)$. We define the distorted-signal-to-noise ratio (DSNR) as follows:

$$\mathrm{DSNR} = 10\log\left\{\frac{\mathrm{var}[\sigma(t)d(t)+m(t)]}{\mathrm{var}[w(t)]}\right\}. \tag{20}$$

The signals $\sigma(t)$ and $m(t)$ were numerically generated using a stationary Markov-1 model. The numerator of Eq. (20) was estimated from the generated data and remained a fixed quantity. The synthetic data $d(t)$ was produced using a pseudo-random binary sequence (PRBS) polynomial with order 15. The length of the data was one period of the PRBS sequence; that is, $2^{15}-1$ bits, and the sampling rate was assumed to be 10 samples per bit. We also used 20 bits per frame. To reduce the effect of the AWGN, an adaptive Wiener filter[10] (AWF) was used. As reported in Ref. 10, the AWF estimates the local mean and variance around each point of the sampled data $r(n)$ as follows:

$$\mu = \frac{1}{N}\sum_{n\in\eta} r(n), \tag{21}$$

$$\sigma^2 = \frac{1}{N}\sum_{n\in\eta} r^2(n) - \mu^2, \tag{22}$$

where η is the N-sample neighborhood of each sample in the signal. The AWF then creates a sample-wise noise-removal filter using these estimates

$$J(n) = \mu + \frac{\sigma^2 - v^2}{\sigma^2}[r(n)-\mu], \tag{23}$$

where v is the average of all of the estimated variances over the block $n\in\eta$. It is noted that when a sample is very different from its neighbors, such as the samples at the bit transition, then $\sigma^2 \gg v^2$, and it follows from Eq. (23) that $J(n)\cong r(n)$. This ensures that the step-wise bit changes are nearly preserved. Accordingly, when the adjacent samples are nearly the same, such as the samples within a bit, then $\sigma^2 \cong v^2$ and consequently, Eq. (23) reveals that in this event

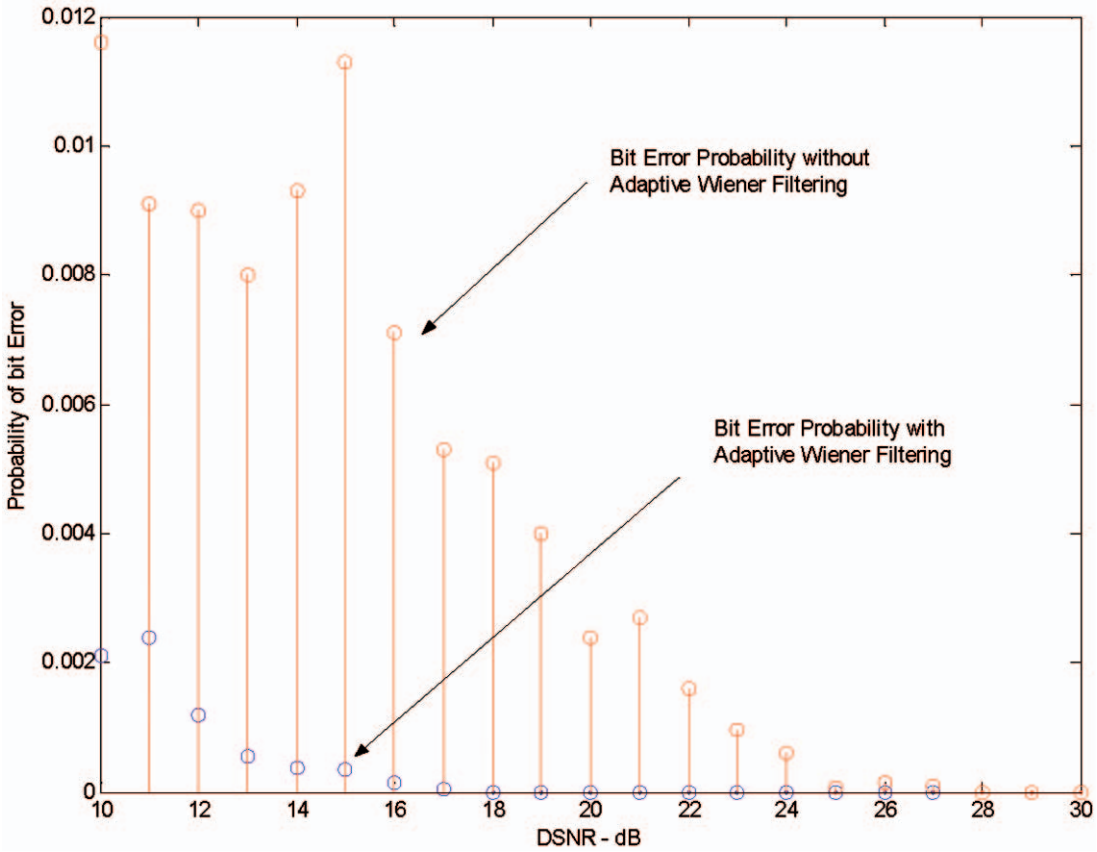

Fig. 11 Probability of bit error versus the distorted signal to noise ratio (DSNR).

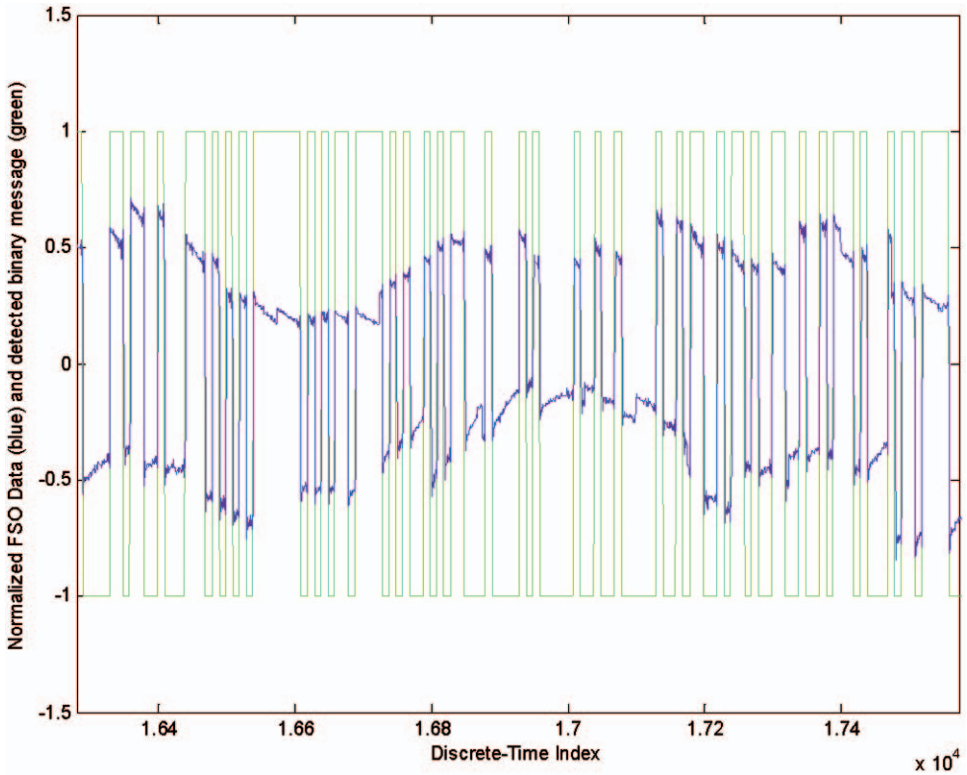

Fig. 12 Portion of the received data and its corresponding detected binary sequence.

$J(n) \cong \mu$. To perform the noise removal as well as preserving the sharp edges of the FSO data, it is best to have, at the most, one bit transition in the moving blocks of the AWF. Clearly, a value of N less than the bit sample number satisfies the prior condition. For this experiment, the bit sample number is 10, therefore we used $N=5$ samples in the experiment. Figure 10 (top) highlights a portion of the data with DSNR=10 dB. This figure (bottom) also illustrates the filtered data using an AWF. This figure shows that the ADF considerably reduces the AWGN while preserving the abrupt bit transitions of the data. Figure 11 illustrates the calculated probability of bit error versus DSNR with and without the AWF. This figure shows that, for the synthetic data generated for this experiment, the AWF is exceedingly successful in reducing the effect of the AWGN. The figure also demonstrates that the probability of bit error is considerably improved using the AWF. Finally, Fig. 12 illustrates a portion of the received data and its corresponding detected binary sequence. This figure indicates that the receiver correctly detects the binary data despite the variations of mean and variance.

7 Summary and Conclusions

In this work, a new method is presented to perform synchronization and detection of binary NRZ data from an FSO communications link. Based on the wavelet transformation, a new filter is developed and presented. The output of the filter is zero mean and is an approximation of the derivative of the binary data. The filter has a zero phase in its band of interest. Therefore, its output is used for synchronization and detection of the data. Analysis of the method is presented using Fourier transformation. In addition, it is illustrated that the adaptive Wiener filter is quite effective in reducing the effect of the AWGN while preserving the sharp edges of the data due to the bit transitions. Simulation experiments are performed and presented using real and synthetic data. The results of the experiments indicate that the Haar wavelet transform and an adaptive Wiener filter are robust and effective methods in dealing with the type of NRZ data from an FSO link such as that obtained from the modulating retroreflector link.

A theoretical determination of the expected bit error rate using the methods presented will be presented at an upcoming SPIE conference. Future work will include acquiring new sets of experimental, digitized data from an MRR FSO link with a new PRBS pattern generator with a mathematically reproducible bit pattern for more extensive postprocessed BER testing of the algorithm, as well as for comparison to existing bit synchronization and detection methods. In addition, current plans are to develop hardware for direct application of this method to an FSO link for further testing without having to digitize and store data for postprocessing.

Acknowledgments

The authors would like to acknowledge the reviewers for their constructive comments. We would also like to thank the U.S. Naval Research Laboratory and the Office of Naval Research for support and use of facilities for this work.

References

1. H. R. Burris, C. Moore, M. Vilcheck, R. Mahon, M. Stell, M. Suite, M. Davis, W. Scharpf, A. Reed, W. Rabinovich, C. Gilbreath, E. Oh, and N. M. Namazi, "Low frequency sampling adaptive thresholding for free-space optical communication receivers with multiplicative noise," *Proc. SPIE* **5160**, 355–368 (2003).
2. H. Burris, A. Reed, N. Namazi, W. J. Scharpf, M. J. Vilcheck, M. F. Stell, and M. R. Suite, "Adaptive thresholding for free-space optical communication receivers with multiplicative noise," presented at IEEE Aerospace Conf. March 9–12, 2002, Big Sky, MT, IEEE.
3. H. Burris, A. Reed, N. Namazi, M. Vilcheck, and M. Ferraro, "Use of Kalman filtering in optical communication systems with multiplicative noise," *Proc. IEEE Intl. Conf. Acoust. Speech Signal Process. (ICASSP'2001)* (2001).
4. G. C. Gilbreath, et al., "Large-aperture multiple quantum well modulating retroreflector for free-space optical data transfer on unmanned aerial vehicles," *Opt. Eng.* **40**(7), 1348–1356 (2001).
5. R. E. Ziemer and R. L. Peterson, *Digital Communications and Spread Spectrum Systems*, Macmillan Publishing Co., New York (1985).
6. R. E. Ziemer and W. H. Tranter, *Principles of Communications, Systems, Modulation and Noise*, 5th ed., John Wiley and Sons, New York (2002).
7. R. M. Rao and A. S. Bopardikar, *Wavelet Transforms: Introduction to Theory and Applications*, Addison Weseley Longman, Inc., New York (1998).
8. D. Datta and R. Gangopadhyay, "Simulation studies on nonlinear bit synchronization in APD-based optical receivers," *IEEE Trans. Commun.* **COM-33**(9), 909–917 (1987).
9. S. K. Mitra, *Digital Signal Processing: A Compute-Based Approach*, 2nd ed., McGraw-Hill Irwin, New York (2001).
10. J. S. Lim, *Two-Dimensional Signal and Image Processing*, pp. 536–540, Prentice Hall, Englewood Cliffs, NJ (1990).

Nader Namazi received his PhD from the University of Missouri-Rolla in 1985. He was with the Michigan Technological University, Houghton, from 1985 to 1992, where he was promoted to the rank of associate professor with continuous tenure. Since 1992, he has been with the Catholic University of America, Washington, D.C., where he is currently a professor and chairman in the Department of Electrical Engineering and Computer Science. He was the editor-in-chief of the *International Journal of Modeling and Simulation* from 1994 to 1996. He is the author of the book *New Algorithms for Variable Time Delay and Nonuniform Image Motion Estimation* (Ablex, 1994). His research interests are in image motion detection and estimation, image sequence filtering/restoration, digital communications, and chemical agent detection and classification. Dr. Namazi is a senior member of IEEE and member of Eta Kappa Nu. He is also the recipient of the Alpha Delta Gamma Teaching Award.

Harris Rayvon Burris, Jr. (**Ray**) received the bachelor's degree in physics from the University of California, Berkeley, and the master's degree and PhD in electrical engineering from the Catholic University of America in Washington, D.C. Dr. Burris is a principal research scientist with Research Support Instruments, Inc. of Lanham, Maryland. He has been at the U.S. Naval Research Laboratory since 1985, both as a government employee and as a contractor to the government. He has been working under contract for the Advanced Technology Branch, Code 8123, of the U.S. Naval Research Laboratory in Washington, D.C. since 1998. His current research interests are free-space laser communications, satellite laser ranging, and Geiger mode avalanche photodiode detectors.

Charles Conner received his PhD in electrical engineering from the Catholic University of America in 1998. His specialties are digital signal and image processing and electronic communications systems. He has held many positions in industry (manufacturing, design, and research and development) and in academia (teaching and research).

G. Charmaine Gilbreath received her BS in physics from Georgia Institute of Technology in 1982, and her MSE in electrical engineering and PhD from The Johns Hopkins University in 1986 and 1989, respectively. She has been with the Naval Research Laboratory (NRL) since 1982. Her specialties are in nonlinear optics, free space optical data transfer, and optical device development. She is the lead principal investigator for NRL's multiple quantum well retromodulator programs.